A Markov Chain Monte Carlo Investigation of Spin Models

Dominic Williamson and James Cummins

9846595 and 9906815

School of Physics and Astronomy
The University of Manchester

2nd Year Theory Computing Report

April 2018

Abstract

Monte Carlo simulations using the Metropolis and Wolff algorithms were used to study the properties of various models. Second order phase transitions were observed in the 2D Ising model and the 3D classical Heisenberg model with critical temperatures of $T_c = 2.275 \pm 0.004\, J/k_B$ and $T_c = 1.459 \pm 0.009\, J/k_B$ respectively. Hysteresis in the 2D Ising model was also investigated. The 2D XY model was studied with vortex phenomena being observed. The helicity modulus was used to calculate the critical temperature of this model as $T_c = 0.898 \pm 0.007\, J/k_B$.

1 Introduction

The Ising model is a model of ferromagnetism consisting of magnetic dipole moments of atomic spins arranged in a lattice. These can take one of two values, up or down, corresponding to the direction in which the magnetic moment points. The up and down spins are represented numerically as $+1$ and -1 respectively. Each spin interacts only with its nearest neighbours. Ernst Ising (1900-1998) gave his name to the model after solving the one dimensional case, for which he found that no phase transition occurs [1]. The two dimensional square lattice Ising model with periodic boundary conditions was later analytically solved by Lars Onsager (1903-1976). Onsager showed that in this case there is a second order phase transition with divergences in the specific heat and magnetic susceptibility [2].

Phase transitions can be identified when the order parameter changes from a non-zero to zero value or vice versa. In the Ising model, the magnetisation is zero above a critical temperature and non-zero below said temperature. To obtain values for the critical temperature the Ising model can be simulated using Monte Carlo methods. These are algorithms that use repeated random sampling to obtain numerical results.

2 Ferromagnetic Phase Transitions

2.1 Ferromagnetism

The magnetic moment of an atom is the result of contributions from the intrinsic spin angular momentum and the orbital angular momentum of its electrons. The total magnetisation of a solid, M, is the sum of each atom's magnetic moment, or *spin*. If the spins point in random directions, their contributions will cancel each other out and M will be approximately zero. However, if the spins align such that many of them point in the same direction there will be a net magnetic moment.

Ferromagnets exhibit permanent magnetic properties due to the presence of domains. Domains are regions where spins align parallel to each other. While initially oriented randomly, domains will experience a torque in the presence of an external magnetic field. The spins will then rotate in order to align with the field and minimise their energy. If the field is later removed the material will remain partly magnetised. This is because work was initially done in rotating the domains, so a field in the opposite direction must be applied to reorient them to their original state [3]. This phenomenon is called hysteresis.

2.2 Phase Transitions

At a critical temperature T_c, a ferromagnet will undergo a phase transition. Below T_c the ferromagnet will be in an ordered state whereas above T_c it will be in a disordered, paramagnetic state. In this paramagnetic state, domains cannot form and spins are randomly aligned. This is because any alignment of spins resulting from the magnetic interactions between neighbouring atoms is overcome by the thermal energy of the system [4]. In this state the order parameter M is zero. Below T_c, the reduced thermal energy allows domains to form and the system becomes more ordered. In this state M is non-zero. As the temperature T is decreased below T_c, domains oriented in the direction of M increase in size at the expense of those less favourably oriented. This continues until, at absolute zero, the entire ferromagnet comprises of a single domain of spins.

The ferromagnetic-paramagnetic phase transition is of second order since the order parameter is continuous at T_c whilst its derivative with respect to T is not. This discontinuous quantity is the magnetic susceptibility χ and is given by

$$\chi = \frac{dM}{dT} = \frac{\langle M^2 \rangle - \langle M \rangle^2}{k_B T} \,, \tag{1}$$

where k_B is the Boltzmann constant and the latter equality results from the fluctuation-dissipation theorem [5]. The total energy of the system E is similarly continuous at T_c whilst its first derivative with respect to T is not. This derivative is the specific heat capacity C where

$$C = \frac{dE}{dT} = \frac{\langle E^2 \rangle - \langle E \rangle^2}{k_B T^2} \,. \tag{2}$$

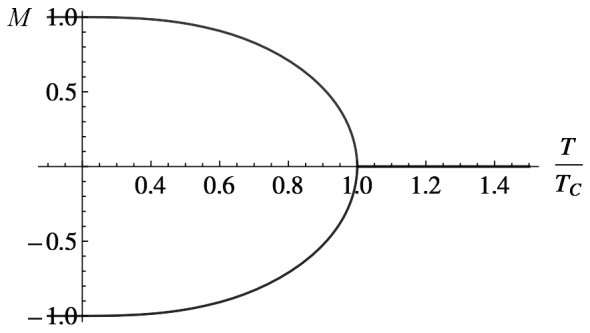

Figure 1: The order parameter M plotted as a function of temperature $\frac{T}{T_c}$. The influence of thermal fluctuations at the transition point determine whether the system acquires a positive or negative magnetisation.

Spontaneous symmetry breaking can be observed at T_c in figure 1 as the bifurcation of the curve. This occurs because above T_c, $M = 0$ and thus the spins S_i are invariant under the rotation $S_i \rightarrow -S_i$. Meanwhile, the non-zero magnetisation below T_c has a direction and is thus no longer rotationally invariant – the symmetry has been broken [6].

3 Algorithms

3.1 Markov Chains

A Markov chain is a sequence of states, such that for a stochastic process, the equilibrium probability of the system being in state X_i is independent of all states but the immediate predecessor [7]. Monte Carlo processes like the Metropolis algorithm use Markov chains where transition probabilities are chosen such that they satisfy the principle of detailed balance,

$$W_{ij} P(X_i) = W_{ji} P(X_j) \,, \tag{3}$$

where W_{ij} is the transition probability to move from state X_i to state X_j and $P(X_i)$ is the equilibrium probability of state X_i [5]. Detailed balance implies that there is no net flow of probability from any one state to another.

3.2 The Metropolis Algorithm

The probability of a given state occurring is dependent on the partition function. In large systems the partition function is not exactly known. This is overcome by generating a Markov chain of

states; if the jth state is produced from the ith state, the relative probability is the ratio of the individual probabilities and the partition function cancels. As a result, only the energy difference ΔE between the two states is required. The Metropolis transition probabilities satisfy detailed balance and are as such [8]:

$$W_{ij} = e^{-\frac{\Delta E}{k_B T}} , \qquad \Delta E > 0 \tag{4}$$

$$W_{ij} = 1 , \qquad \Delta E < 0 . \tag{5}$$

One sweep of the Metropolis algorithm is described by the following steps:

1. Select a random spin in the $L \times L$ lattice
2. Calculate the energy change ΔE which results if the selected spin is flipped
3. If $\Delta E < 0$, flip the spin and go to step (1). Otherwise go to step (4)
4. Generate a random number r such that $0 < r < 1$
5. If $r < e^{-\frac{\Delta E}{k_B T}}$, flip the spin
6. Repeat steps (1) to (5) until L^2 iterations have been completed.

3.3 The Wolff Algorithm

Due to large thermal fluctuations that arise near T_c, the number of sweeps of the Metropolis algorithm required to equilibrate the system increases substantially. This problem, referred to as critical slowing down, is overcome by using a cluster algorithm. Instead of flipping a single spin at a time, cluster algorithms build virtual clusters consisting of a select amount of spins and flip the entire cluster. The Wolff algorithm, demonstrated in figure 2, is an efficient cluster algorithm whereby bonds are introduced between any two parallel nearest neighbour spins. The probability p that a bond exists is given by

$$p = 1 - e^{\frac{2J}{k_B T}} , \tag{6}$$

where J is the coupling parameter between adjacent atoms [9]. One sweep of the Wolff algorithm is summarised as follows:

1. Select a random spin in the lattice
2. Choose a nearest neighbour spin and generate a random number r. If $r < p$, a bond exists between the two spins, and the nearest neighbour spin becomes part of the cluster. Otherwise, this bond is not tested again
3. If a spin is added to the cluster, add its nearest neighbour spins to the list of nearest neighbour spins of the cluster
4. Repeat steps (2) and (3) until no nearest neighbour spins remain
5. Flip all the spins in the cluster
6. Repeat steps (1) to (5) until L^2 iterations have been completed.

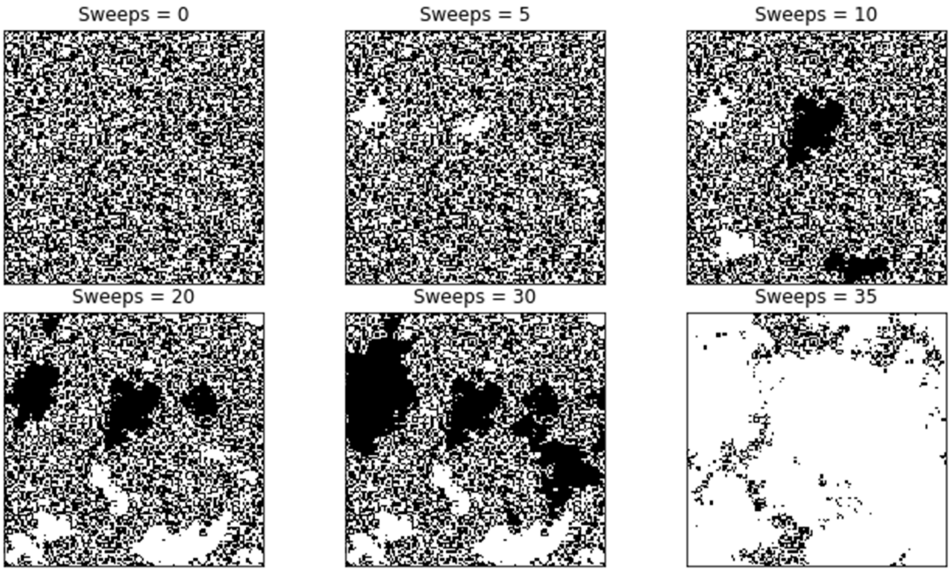

Figure 2: The magnetisation at each point in an $L = 64$ lattice at $\frac{k_B T}{J} = 0.5$ is visualised after incremental numbers of sweeps of the Wolff algorithm, where the white and black pixels represent spins of $+1$ and -1 respectively.

3.4 Periodic Boundary Conditions

To simulate infinite systems with models of finite size, periodic boundary conditions can be used. The boundaries are effectively eliminated by mapping the d-dimensional lattice onto a $(d+1)$–dimensional torus. However, the system is still characterised by the finite lattice size L; hence, the properties of the system differ from those of the corresponding infinite lattice.

4 The 2D Ising Model

4.1 Simulating the Ising Model

The Hamiltonian of the 2D Ising model is given by

$$\mathscr{H} = -J \sum_{\langle ij \rangle} S_i S_j - H \sum_i S_i \ , \tag{7}$$

where $\langle ij \rangle$ denotes the summation over all nearest neighbour pairs, S_i is the ith spin and H is the external magnetic field [2]. In the case $H = 0$, $\mathscr{H}$ is minimised when each spin is aligned with those of its nearest neighbours. Using equation 7, the 2D Ising model was simulated using the Wolff algorithm for varying lattice sizes with $H = 0$.

An initial state of random spins was used. The system was allowed to reach thermal equilibrium before χ and C were calculated – characterised by when E and M had both stabilised. This equilibration was achieved by calculating averages for E and M using moving bins: when the average from the last 100 sweeps had come within 0.001 of the average from the previous 100 sweeps, the system was determined to have equilibrated. It was found that this was the minimum bin size required for E and M to reach their global, rather than just local, stable values at each temperature. Once the system had equilibrated, 256 further sweeps were performed to measure the average values of E and M. χ and C were then calculated using equations 1 and 2 respectively. This process was repeated for decreasing T, reusing the previous spin configuration before each

new temperature. This reduced the time taken for the system to equilibrate. The graphs of $\langle E \rangle$, $\langle M \rangle$, χ, and C were plotted as seen in figure 3.

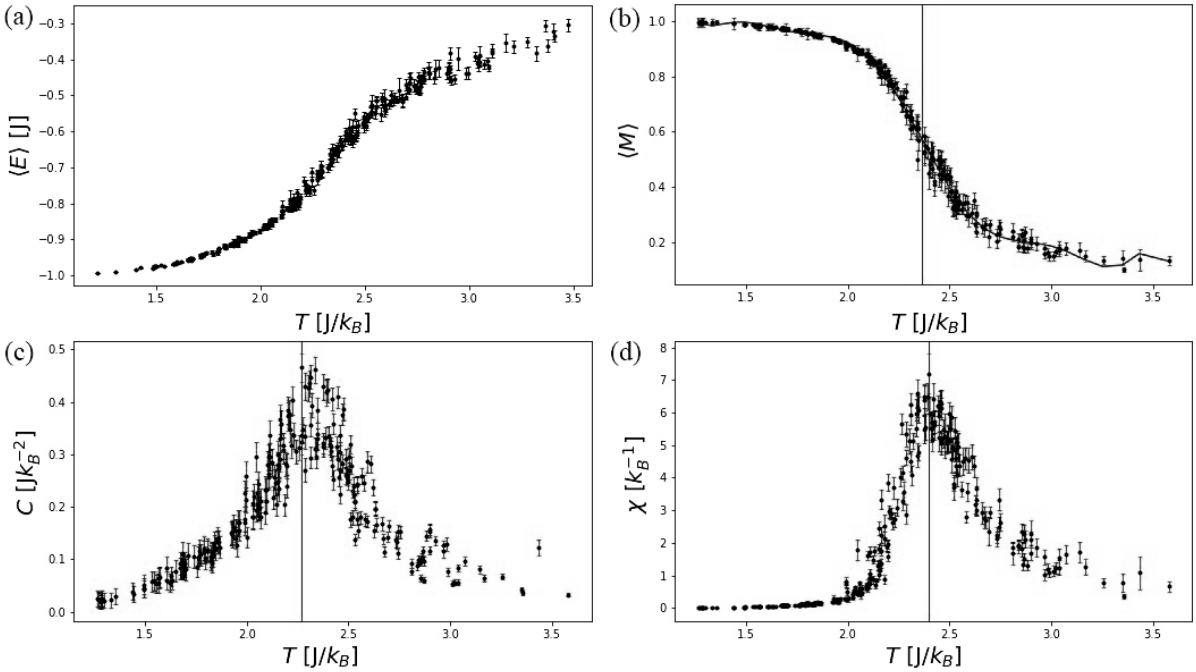

Figure 3: Plots of (a) the average energy per site, (b) the magnitude of the magnetisation per site, (c) the specific heat capacity and (d) the magnetic susceptibility as functions of temperature. A range of 256 temperature points were selected by sampling a normal distribution of standard deviation 0.5 about an estimate of T_c obtained in an earlier run. An $L = 16$ lattice is illustrated here with vertical lines corresponding to the value of T_c for each graph.

4.2 Time Correlation

Due to the central limit theorem, the data for each quantity may be assumed to be normally distributed if the sample consists of a considerable number of independent measurements [10]. In order to obtain independent measurements, the correlation length ζ must be considered. ζ describes how strongly spins at different locations in the lattice are correlated. As T_c is approached, ζ diverges to infinity and the probability of consecutive measurements being statistically independent becomes zero [11]. For an observable A, the autocorrelation function ρ_A quantifies the correlation between measurements taken at different times. ρ_A can be used to calculate a correlation timescale τ_A, after which new measurements will be uncorrelated and therefore independent. The normalised autocorrelation function between two times t and t' is given by

$$\rho_A(t,t') = \frac{\langle (A(t) - \langle A \rangle)(A(t') - \langle A \rangle) \rangle}{\langle A^2 \rangle - \langle A \rangle^2} \,, \tag{8}$$

where $\rho_A = 1$ corresponds to the maximum possible correlation. Since any two measurements become completely independent for $(t' - t) \to \infty$, ρ_A will tend to zero in this limit. Furthermore, it can be shown that ρ_A decays exponentially with time, especially for large time intervals, except at T_c. In non-cluster algorithms such as the Metropolis algorithm, the correlation timescale diverges at T_c [12]. The Wolff algorithm ensures that the divergence of τ_A is averted. It was therefore possible to determine τ_A within each simulation run by measuring the time taken for ρ_A to decrease to successive reciprocal powers of e. The value these time intervals converged toward was assigned to τ_A.

4.3 Error Determination

The correlation time was used to determine the errors via the bootstrap binning method. This is where n random bins are created from N, not necessarily independent, data points. The average values of A are calculated for each bin from which $\langle A \rangle$ and $\langle A^2 \rangle$ are determined. These are used to obtain an estimate for the error on A, σ_A, with [12]

$$\sigma_A = \frac{1}{L}\sqrt{(1+2\tau_A)(\langle A^2 \rangle - \langle A \rangle^2)}\,. \tag{9}$$

A value of $n = 1000$ was used because this was found, through an iterative process, to be the point at which the errors on each observable had converged towards stable values.

4.4 The Critical Temperature

To determine T_c, polynomial regression was used to find the point of maximum gradient for M. This technique was used since around T_c, M varies as

$$M(T) \propto \left|\frac{T - T_c}{T_c}\right|^{\nu}\,, \tag{10}$$

where $\nu > 0$ is a critical exponent [5]. Thus M may be approximated by a polynomial expansion of equation 10. Through incremental testing, it was found that the sum of squared residuals converged for polynomials of order 9 – therefore this degree was used in the regression analysis. The error on T_c was determined using

$$\sigma_{T_c} = \frac{1}{N}\sqrt{\sum_i r_i^2}\,, \tag{11}$$

where r_i are the residuals of the fit and N is the number of data points. E was not used to determine a value for T_c because, unlike M, around T_c it does not follow a scaling relation with $\left|\frac{T-T_c}{T_c}\right|$. To determine T_c from the graphs of χ and C, the maximum measurements of each quantity were used since they diverge at the transition point. The errors on these values for T_c were determined to be the temperature difference from the maxima of each graph to the next highest data point.

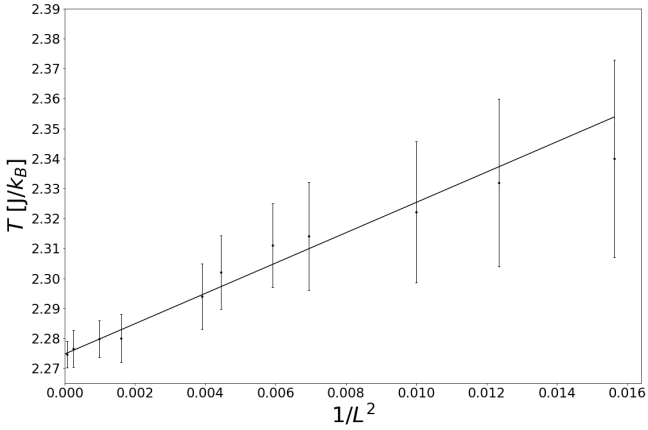

Figure 4: The weighted averages of the critical temperatures plotted as a function of the reciprocal lattice size, where finite-size scaling has been used to extrapolate the regression line to find T_c for a lattice of infinite size. The linear fit has a χ^2_{red} of 0.369.

Since the lattices are of finite size, no true phase transition occurs in the simulations. This is illustrated by the continuity of χ and C at T_c in figure 3. Finite-size scaling is thus used whereby

values of T_c are plotted against the reciprocal lattice sizes as shown in figure 4. Linear regression is then used to extrapolate to zero, producing the value of T_c for an infinite lattice [5]. Using this technique, the critical temperature of the 2D Ising model for an infinite lattice was calculated to be $T_c = 2.275 \pm 0.004\ J/k_B$.

4.5 Hysteresis

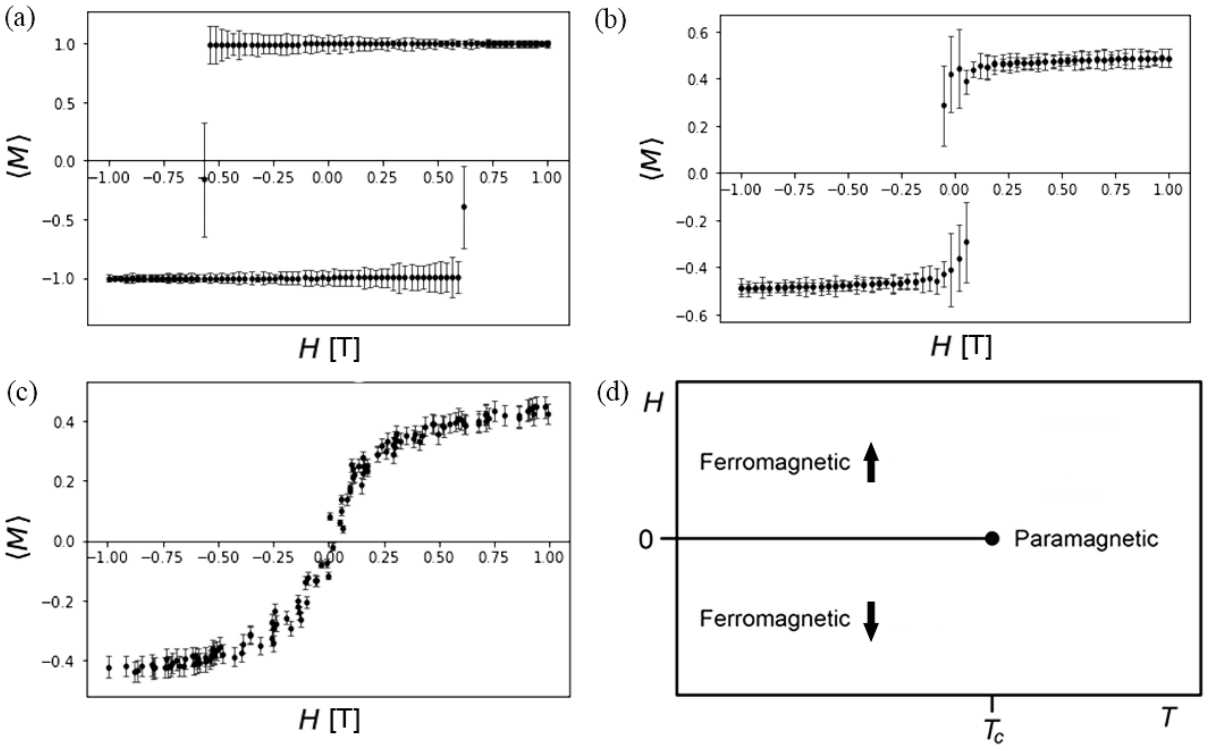

Figure 5: Graphs (a), (b), and (c) show the response of M to a varying external magnetic field for $\frac{k_B T}{J} = 1$, $\frac{k_B T}{J} = 2$, and $\frac{k_B T}{J} = 3$ respectively. The phase diagram in (d) illustrates how varying T and H alters the magnetisation properties of the system.

An oscillating external magnetic field H was applied to the system and hysteresis was observed. For $T < T_c$, M is discontinuous at the points $H = \pm H_c$ as shown in figure 5a. H_c is the coercive field strength and is defined as the magnetic field required to orient the domains such that the system becomes demagnetised. Varying the field strength about $\pm H_c$ produces an abrupt change in M, especially for $T << T_c$ when there are fewer, larger domains. Thus this small variation yields a phase transition. This is a first order transition, defined as where the order parameter is discontinuous at the transition point [6].

As T_c is approached, H_c becomes smaller in magnitude, which is seen by comparing figures 5a and 5b. This occurs because as T increases, the average size of the domains becomes smaller. As a result the strength of the magnetic field required to demagnetise the system decreases. The size of the discontinuity also decreases since M is smaller when closer to T_c. Above T_c, M is approximately zero and the system only experiences an induced magnetism. Hence in the paramagnetic state, M transitions smoothly as H is varied and no hysteresis is observed as illustrated in figure 5c [13]. The phase diagram in figure 5d encapsulates how the 2D Ising model responds to variations in H for different T.

5 The 2D Classical XY Model

The 2D Ising model can be generalised such that the spins are able to rotate in the plane of the lattice. This is called the 2D classical XY model. In the case $H = 0$ the Hamiltonian is given by

$$\mathscr{H} = -J \sum_{\langle ij \rangle} \vec{S}_i \cdot \vec{S}_j \ , \tag{12}$$

where $\vec{S}_i$ is the spin vector of the ith spin. The spin vectors are of unit length and are each characterised by an angle corresponding to the direction in which the spin points. The Mermin-Wagner theorem states that no phase transition occurs in the 2D XY model; however, there is a Kosterlitz-Thouless (KT) transition [14]. At low temperatures most spins are aligned and ζ decays as a power law. At high temperatures ζ decays exponentially. At the critical temperature the KT transition between these two phases occurs. The transition can be identified using the helicity modulus Υ. The helicity modulus is a measure of the change in energy due to a rotation of the spins and is given by

$$\Upsilon = -\frac{1}{2}\langle E \rangle - \frac{1}{T}\left\langle \left(\sum_{\langle ij \rangle} \sin(\theta_i - \theta_j) \vec{r_{i,j}} \cdot \vec{x} \right)^2 \right\rangle , \tag{13}$$

where θ_i is the angle of the ith spin, $\vec{r_{ij}}$ is the vector from spin i to j and $\vec{x}$ is an arbitrary unit vector. It can be shown that in the limit $T \to T_c$, $\Upsilon/T = 2/\pi$. Therefore the intersection of the lines $y = \Upsilon$ and $y = 2T/\pi$ yields the critical temperature [15].

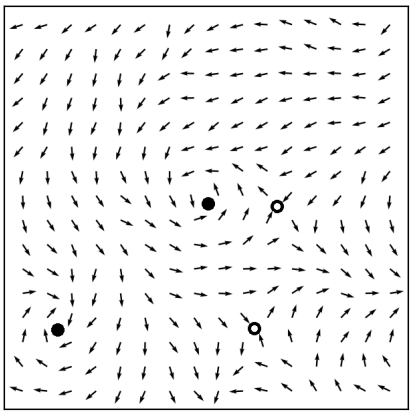

Figure 6: Vortices are shown as solid circles and antivortices are shown as white circles with a black perimeter. They are able to move through the lattice and upon meeting a vortex-antivortex pair will annihilate. This is analogous to the Coulomb interaction between electric point charges.

Using the Metropolis algorithm a square lattice with periodic boundary conditions was investigated. Topologically stable formations in which regions of spins rotate about a full circle were observed as seen in figure 6. These can rotate clockwise, a vortex, or anticlockwise, an antivortex. It can be shown using Stokes' theorem that the number of vortices and antivortices is always equal. Adding vortex-antivortex pairs into the system requires energy which is provided by thermal fluctuations. As a result, more pairs occur the greater the temperature [14]. The critical temperature for varying lattice sizes was determined using the helicity modulus as shown in figure 7. The critical temperature for an infinite lattice was calculated as $T_c = 0.898 \pm 0.007 \, J/k_B$ from finite-size scaling. Unlike the Ising model, in order for the XY model to become disordered, the spins need not be antiparallel but only sufficiently misaligned relative to one another. Given

that, in an ordered system, the thermal energy required to flip a binary spin is greater than that required to reorient a continuous spin by an angle $\theta < \pi$, we postulate that this justifies the smaller critical temperature of the 2D XY model relative to the Ising model.

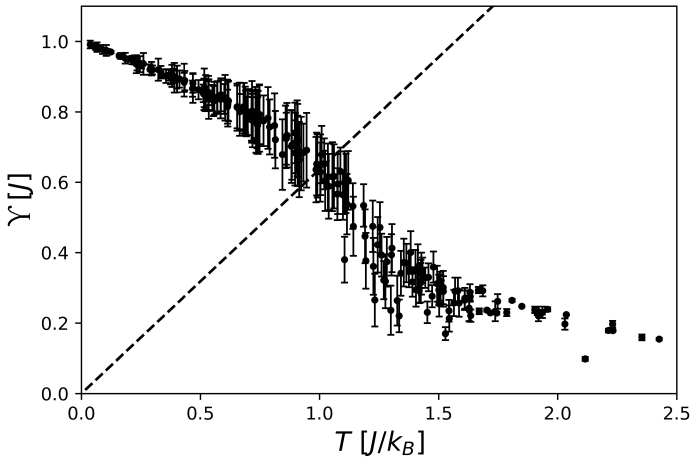

Figure 7: Temperature points were generated by sampling a normal distribution of standard deviation 0.6. An $L = 16$ lattice is shown here with errors on each data point and T_c calculated using the bootstrap binning method and equation 11, respectively.

6 The 3D Classical Heisenberg Model

In the 3D classical Heisenberg model the spins are arranged in a 3D lattice and can point in any direction in three dimensional space, as illustrated in figure 8. The Hamiltonian in the case $H = 0$ is given by equation 12. A 2D, $6 \times L^3$ array was used to represent the cubic lattice. The Metropolis algorithm was used to measure E, M, χ and C. A second order phase transition was observed in the order parameter M. Using finite size scaling, the critical temperature of this model was found to be $T_c = 1.459 \pm 0.009\ J/k_B$. The difference between this value and that of the 2D Ising model is thought to be a consequence of the increased number of nearest neighbours. As a result of this, the total magnetic interaction between spins in the 3D lattice is greater and therefore the magnitude of the thermal excitations required to overcome them increases.

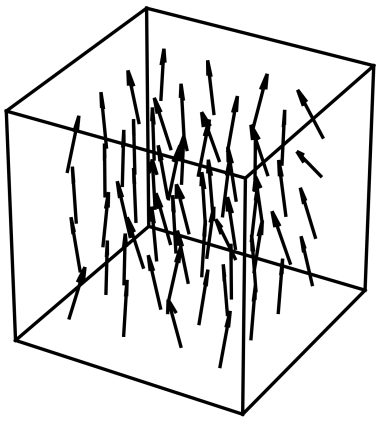

Figure 8: The result of a $L = 4$ cubic lattice at $T = 0.1\ J/k_B$ after 20 sweeps of the Metropolis algorithm. Once the system equilibrated, $\langle E \rangle$, $\langle M \rangle$, χ and C were measured. Errors on each data point and T_c were determined using the methods described in section 4.4.

7 Conclusion

The value of T_c determined for the 2D Ising model is 1.500 standard deviations from the analytical value of 2.269 J/k_B [2]. Compared to results obtained by another study T_c is 0.857 standard deviations from the studies value of 0.892 J/k_B for the 2D classical XY model [16]. Likewise, T_c is 1.777 standard deviations from another studies value of 1.443 J/k_B for the 3D classical Heisenberg model [17]. A continuation of the study of spin systems would be to consider a model in which the spins can point freely in 4 dimensions. This would act as a simple model for the class of particles that are responsible for the Higgs mechanism [18].

References

[1] Ising, E., "Beitrag zur Theorie des Ferromagnetismus", *Zeitschrift fur Physik*, volume 31, 1925, pp. 253.

[2] Onsager, L., "Crystal Statistics. I. A Two-Dimensional Model with an Order-Disorder Transition", *Phys. Rev.*, volume 65, 1944, pp. 117.

[3] Feynman, R.P., Leighton, R.B., Sands, M., *The Feynman Lectures on Physics*, volume 2, Basic Books, Perseus Books Group, New York, 2010, section 37.

[4] Hook, J.R., Hall, H.E., *Solid State Physics*, John Wiley & Sons Ltd., Chichester, 2nd edition, 2004, p. 220.

[5] Landau, D.P., Binder, K., *A Guide to Monte Carlo Simulations in Statistical Physics*, Cambridge University Press, Cambridge New York, 3rd edition, 2009, chapter 4.

[6] Selinger, J.V., *Introduction to the Theory of Soft Matter*, Springer International Publishing, 2016, pp. 7.

[7] Markov, A.A., "Extension of the Law of Large Numbers to Quantities", *Izvestiia Fiz. Mat. Obschestva Kazan University*, volume 2, 15, 1906, pp. 135.

[8] Metropolis, N., Rosenbluth, A.W., Rosenbluth, M.N., Teller, A.H., Teller, E., "Equation of State Calculations by Fast Computing Machines", *The Journal of Chemical Physics*, volume 21, 6, 1953, pp. 1087.

[9] Wolff, U., "Collective Monte Carlo Updating for Spin Systems", *Phys. Rev. Lett.*, volume 62, 1989, pp. 361.

[10] Billingsley, P., *Probability and Measure*, John Wiley & Sons Ltd., New York, 3rd edition, 1995, pp. 357.

[11] Chen, W., Legner, M., Rüegg, A., Sigrist, M., "Correlation Length, Universality Classes, and Scaling Laws Associated with Topological Phase Transitions", *Phys. Rev. B*, volume 95, 2017, p. 75116.

[12] Anagnostopoulos, K.N., *Computational Physics*, National Technical University of Athens, Athens, 2016, pp. 537.

[13] Giordano, N.J., Nakanishi, H., *Computational Physics*, Pearson Education Inc., 2nd edition, 2005, pp. 259.

[14] Kosterlitz, J.M., Thouless, D.J., "Ordering, Metastability and Phase Transitions in Two-Dimensional Systems", *Journal of Physics C: Solid State Physics*, volume 6, 7, 1973, p. 1181.

[15] Van Himbergen, J.E., Chakravarty, S., "Helicity Modulus and Specific Heat of Classical XY Model in Two Dimensions", *Phys. Rev. B*, volume 23, 1981, pp. 359.

[16] Olsson, P., "Monte Carlo Analysis of the Two-Dimensional XY Model. II. Comparison with the Kosterlitz Renormalization-Group Equations", *Phys. Rev. B*, volume 52, 1995, pp. 4526.

[17] Peczak, P., Ferrenberg, A.M., Landau, D.P., "High-Accuracy Monte Carlo Study of the Three-Dimensional Classical Heisenberg Ferromagnet", *Phys. Rev. B*, volume 43, 1991, pp. 6087.

[18] Kuti, J., Lin, L., Shen, Y., "Fate of the Standard Model with a Heavy Higgs Particle", *Nuclear Physics B - Proceedings Supplements*, volume 4, 1988, pp. 397.